

# ABOUT THE MICROPOROSITY OF SOME ACTIVATED CARBONS

*S. Duber (1,2), J.N. Rouzaud (3) and C. Clinard (3)*

1. *Institute of Coal Chemistry, Polish Academy of Sciences,  
ul. Sowinskiego 5, 44-102 Gliwice, Poland*

2. *University of Silesia, Faculty of Earth Sciences,  
ul. Bedzinska 60, 41-200 Sosnowiec, Poland*

3. *Centre on Divided Matter, CNRS-Orléans University,  
1<sup>B</sup> rue Férollerie, 45071-Orléans Cédex 2 , France*

## Introduction

Activated chars are usually poorly organised and the exact nature of their micropores is always strongly discussed. Moreover, as shown by High Resolution Transmission Electron Microscopy (HRTEM), the classical models based on spherical or cylindrical pores appear as simplistic. This casts some doubts on the results obtained by classical methods to study the porosity such as gas adsorption. Our approach is thus to obtain quantitative data on the organisation of such microporous carbons, in order to revisit the concept of microporosity. We elaborate activated carbon from a pure and homogeneous saccharose-based char. Their multiscale organisation (structure and microtexture) was directly imaged by HRTEM. An image analysis procedure was developed on our HRTEM images to obtain quantitative data. Results obtained on optical properties (reflectance measurements) will be discussed with HRTEM data in order to precise the microporosity development during the activation process.

## Experimental

A saccharose-based coke was obtained by pyrolysis up to 1000°C under nitrogen flow. This raw char was activated by CO<sub>2</sub> at 850°C. The activation durations were : 2, 5, 10 and 20 hours.

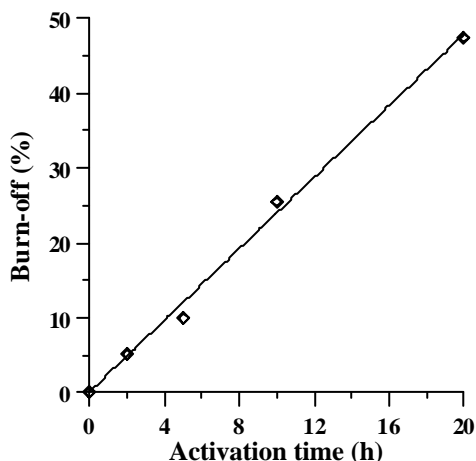


Figure 1a. Burn-off versus activation time

The burn-off obtained after 20 hours activation reaches about 50 % (Figure 1a). Such activation conditions lead to a strong increase of the specific surface areas : from 20 m<sup>2</sup>/g for the raw char to more than 1200 m<sup>2</sup>/g for the most activated char (Figure 1b). The multiscale organisation (structure and microtexture) of these chars was studied by High Resolution Transmission Electron Microscopy (HRTEM), thanks to a Philips CM 20 microscope, operating at 200 kV. A lab-made image analysis procedure was especially developed for such poorly organised carbons. Thanks to this procedure (see Figure 4), quantitative structural and microtextural data can be extracted [1,2].

Reflectance measurements were performed with an Axioskop MPM 200 (Opton) optical microscope in reflected polarized light. The Kilby crossplots (bireflectance vs apparent extreme reflectances) were used in order to precise the optical character of the reflectance ellipsoid called Reflectance Indicating Surface (RIS) [3]. Characteristic parameters, such as their uniaxiality or biaxiality, and their sign, positive or negative, were extracted from this RIS [3]. For heterogeneous carbon materials, optical classes can be determined by a numerical approach carried out on these crossplots, according to a method we developed [4].

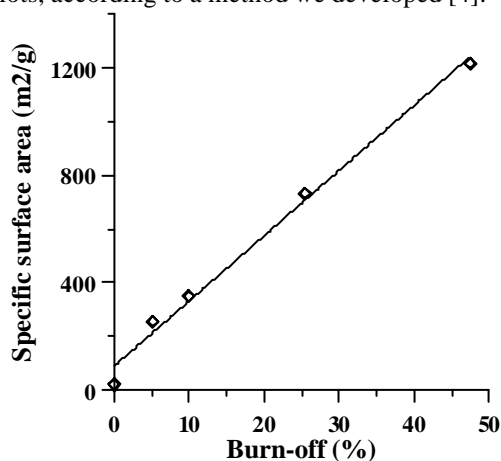


Figure 1b. Specific surface area versus burn-off

## Results

### HRTEM data

The raw coke is formed of aromatic layers of nanometric size. They are often single layers (about the half of the layers), but they can be piled-up by 2 or 3 to give Basic Structural Units (BSU). The large interlayer spacing and the misorientation of the layers is responsible for the material microporosity. These layers or BSU are locally oriented in parallel to form small domains, less than 5 nm in size. Such multiscale organisation is imaged in the Figure 2.

Unexpectedly, the major part of each of the activated chars do not show very striking differences with the raw char, despite the large increase of the BET specific surface areas. After activation, the char becomes more and more heterogeneous. However, within a mainly unmodified char, noticeable changes can be observed in some areas (probably the exterior part of the activated particles, directly submitted to the CO<sub>2</sub>). These strongly activated parts are much less compact. They contain a larger amount of continuous but distorted single layers as shown in the Figure 3. Some burnt areas could form some mesopores, a few nanometers wide.

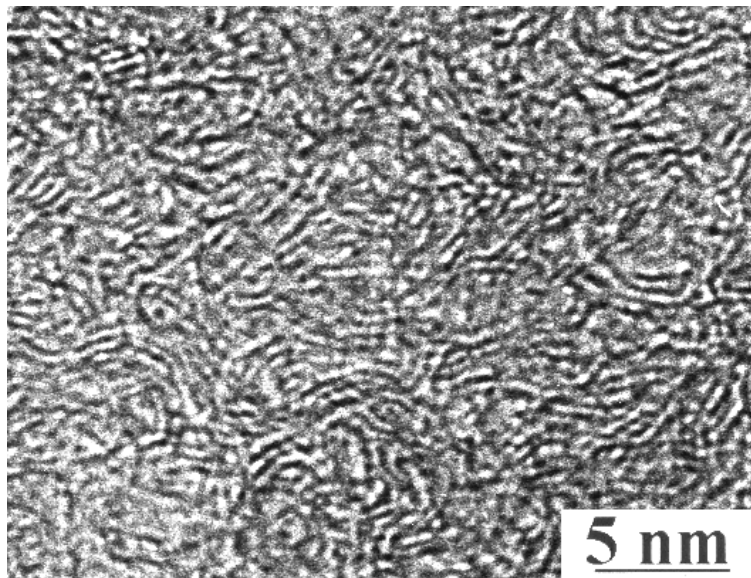


Figure 2: HRTEM images of the raw saccharose-based char.

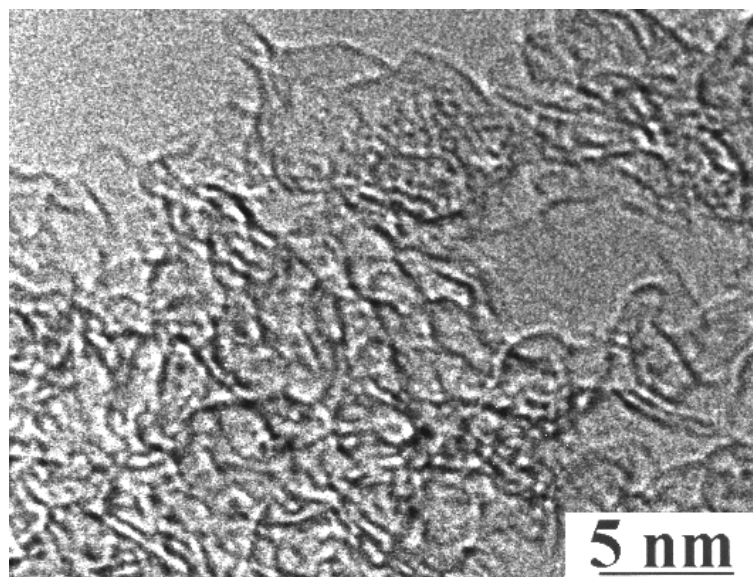


Figure 3 : HRTEM images of the most activated parts of the same sample after 20 h activation under CO<sub>2</sub> flow at 850°C.

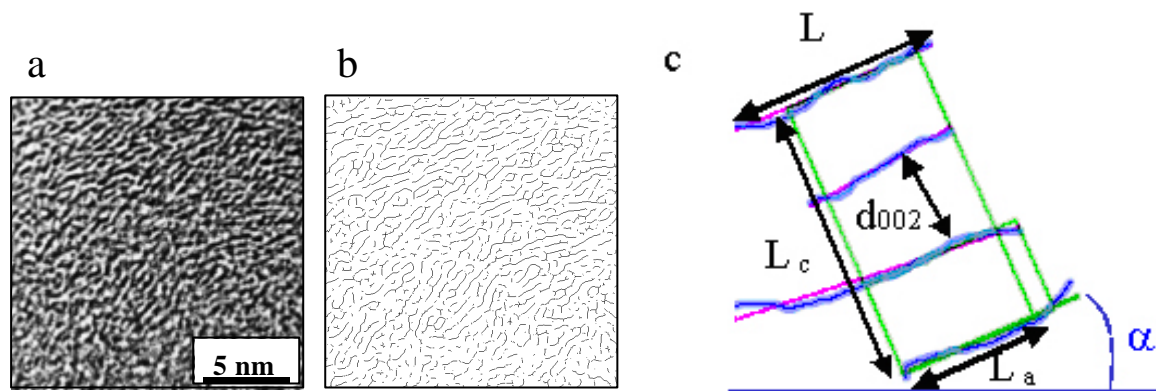


Figure 4. a : raw HRTEM image ; b : skeletonized HRTEM image from a  
 c : structural and microtextural analysis :  
 profile of the aromatic planes (in blue), limits of a coherent domains (in green),  
 definition of the structural ( $L$ ,  $L_a$ ,  $L_c$ ,  $N$  et  $d_{002}$ ) and microtextural parameters (?)

An in-house image analysis procedure was developed in order to obtain the quantitative structural and microtextural data required for a more complete interpretation of these complex images [1,2]. We adopt the following procedure : background noise reducing (filtration of the Fourier Transform), thresholding and binarisation, skeletonization and computerised extraction of quantified structural and microtextural data. So, can be determined :  $L$ , the fringe lengths,  $d_{002}$  the interlayer spacings,  $L_a$  and  $L_c$  respectively the width and the height of the coherent domains,  $\alpha$  the angle of each fringe with a reference direction. For such disordered carbons, we considered a pair of fringes as two single planes when their misorientation was more than  $15^\circ$  and/or their spacing larger than  $7 \text{ \AA}$ , value above which the Van der Waals forces can be neglected.

In the saccharose-based char observed before activation, the amount of single layers is about 42 %, the mean layer length  $L$  is  $8.7 \text{ \AA}$ , the mean domain width  $L_a$  is  $4.5 \text{ \AA}$ , whereas the mean interlayer spacing  $d_{002}$  is  $4.7 \text{ \AA}$ . After activation, the data become strongly scattered according to the studied area. After 20 h activation, as previously observed on the micrographs, the amount of single layer increases to 53 % and locally reaches more than 75 %.  $d_{002}$  slightly increases to a mean value of  $4.9 \text{ \AA}$  and is larger than  $5.5 \text{ \AA}$  in the most activated parts.  $L$  values decreases up to  $8.2 \text{ \AA}$  and mean values of  $6.5 \text{ \AA}$  are brought out in the most burnt areas. Consequently, activation correspond to a burn-off of the smallest and most distorted layers, responsible for a slight increase of the interlayer spacing and a strong increase of the single layers. Slit-shaped micropores develop; they could be described as pairs of spaced layers.

#### Reflectance data.

Measurements of bireflectances (difference between apparent maximum and minimum reflectances of a given section) were first performed on randomly oriented char grains. Mean maximum and minimum reflectance can be calculated. Thanks to an original method developed by Kilby [3], it is possible to reconstruct the reflectance ellipsoid, called Reflectance Indicating Surfaces (RIS), from the couples of apparent maximum and minimum reflectances of a given section ( $R'_{\max}$ ,  $R'_{\min}$ ) plotted versus the apparent bireflectance ( $R'_{\max} - R'_{\min}$ ) (Kilby's crossplots).

This allows us to determine the true values of  $R_{\text{MAX}}$  the maximum reflectance and  $R_{\text{NT}}$  and  $R_{\text{MIN}}$ , respectively the intermediate and minimum reflectances. Optical characteristics of the RIS such as  $R_{\text{ev}}$ , the radii of a sphere with the same volume than the RIS, can be determined. The type and the degree of anisotropy of the carbon can be then specified [3].

With an increasing activation, the apparent maximum reflectances  $R'_{\max}$  and the apparent minimum reflectances  $R'_{\min}$  decrease (see Figure 5 a and b). From these data, the Kilby's crossplots can be constructed. The crossplots obtained for the raw char and for the highly activated char (during 20 hours) are respectively given the figures 5a and 5b. They show that, for an increasing activation, the reflectance decrease is coupled to a strong increase of the char heterogeneity (note the strong point scattering in figure 5b); this well agrees with the TEM observations. Due to this char heterogeneity, the calculations according to the Kilby's procedure becomes impossible, and a new method adapted for heterogeneous carbons was proposed by Duber *et al* [4]. This numerical approach carried out on the Kilby's crossplots permits to separate different optically homogeneous classes within a heterogeneous carbon; their RIS parameters can be then determined and a coefficient of heterogeneity can be calculated (zero for an homogeneous carbon, more than 5 for a very heterogeneous one). This method was applied here and the main results obtained for an increasing activation are given in the table.

For longer and longer activation times, and thus for increasing burn-off and specific surface areas,  $R_{\text{MIN}}$ ,  $R_{\text{INT}}$  and  $R_{\text{MAX}}$  decrease as shown in the Figure 6 where the BET surface area is plotted versus  $R_{\text{MAX}}$ . Whereas  $R_{\text{ev}}$  decreases from 5.3 to 3.2 (Figure 7), the Kilby parameters describing the RIS anisotropy do not significantly change during activation and these chars can be considered as slightly negative biaxial ( $R_{\text{st}}$  about -18). By the Duber procedure, the heterogeneity can be specified : the number of optical classes passes from 3 in the raw char to 13 for 20 hours activation. Whatever the activation duration, all these classes usually correspond to rather isotropic materials.

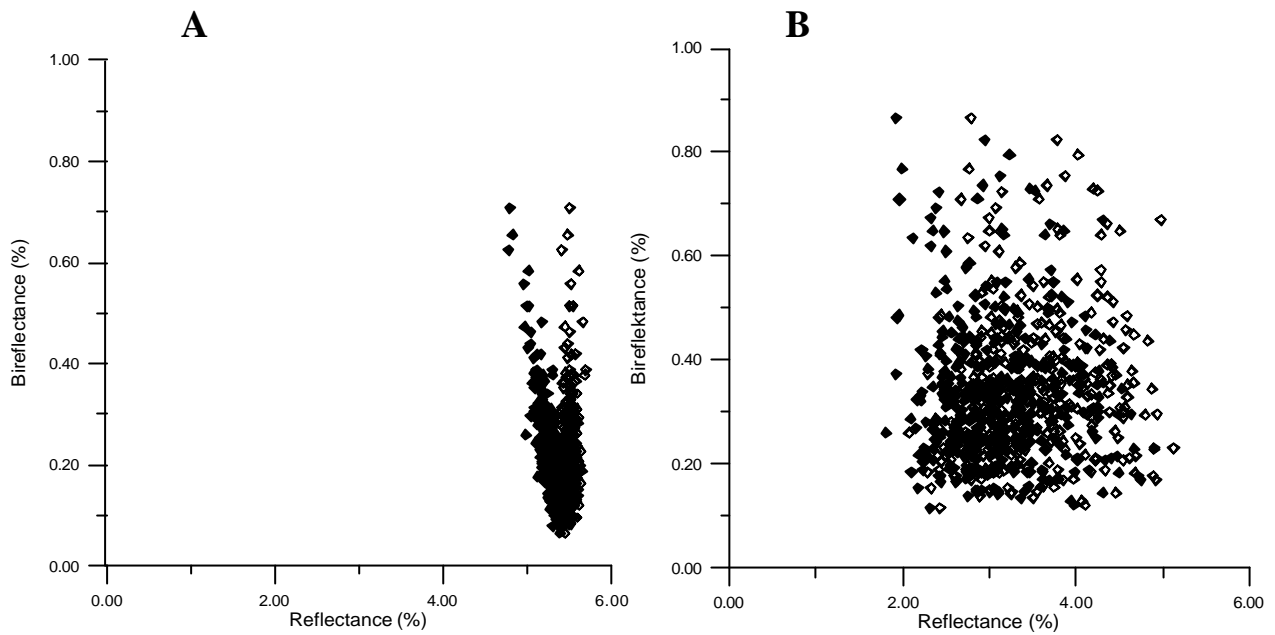


Figure 5. Kilby's crossplots of the saccharose-based chars: (a): before activation; (b) ; after 20 hours activation (full squares : apparent minimum reflectance values; empty squares : apparent maximum reflectance values)

Activation time (h)	$R_{MAX}$	$R_{INT}$	$R_{MIN}$	$R_{ev}$	Heterogeneity Coefficient
0	5.6	5.4	4.8	5.27	0.01
2	5.8	5.5	4.7	5.29	0.05
5	5.4	5.2	4.6	5.06	0.44
10	4.8	4.7	4.1	4.52	2.81
20	3.6	3.4	2.8	3.21	6.70

Table. Optical characteristics ( $R_{MAX}$  : mean maximum reflectance,  $R_{INT}$  : mean intermediate reflectance,  $R_{MIN}$  : mean minimum reflectance,  $R_{ev}$  : equivalent reflectance and heterogeneity coefficient).

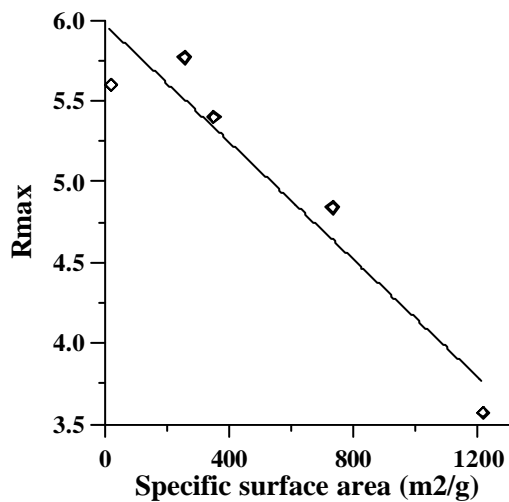


Figure 6. BET specific surface area versus  $R_{MAX}$

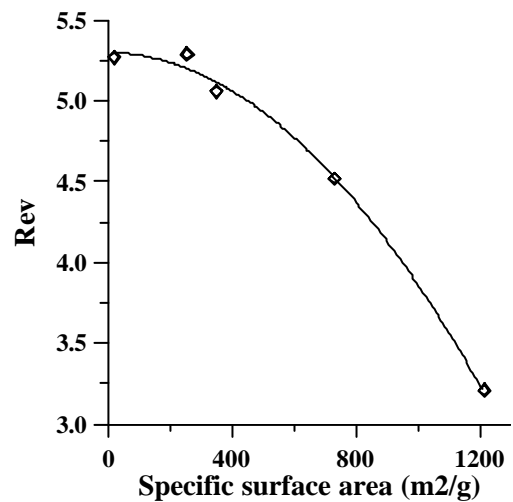


Figure 7.  $R_{ev}$  versus the BET specific surface area

## Discussion - Conclusion

CO<sub>2</sub> activation of a saccharose-based char leads to strong modifications of its optical properties. A higher burn-off leads to larger BET surface areas and increasing porosity, as shown by HRTEM. All the reflectance values decrease with the activation duration, i.e. with the porosity increase (see table and figures 6 and 7). Consequently, the progress of the activation process, can be easily characterized by following the reflectance data evolution, as already proposed by Jagtoyen *et al* for coal-based adsorbent carbons [6]. In the present work, and as far as the saccharose-based porous carbons are concerned, the increase of the BET specific surface area can be followed by  $R_{ev}$  measurements.

As shown by HRTEM, the classical models based on spherical or cylindrical pores appear as simplistic, whereas the slit-shaped micropores could be more realistic. This casts some doubts on the results obtained by classical methods to study the porosity such as gas adsorption and Small Angle X ray Scattering, since they usually imply assumptions on simplistic pore shape. The image analysis procedure we developed for these poorly organized carbons allows to obtain pertinent structural parameters. Despite the very strong heterogeneity of the activated chars, it appears that activation induces the burn-off of the smallest and the most distorted layers. This leads to an higher amount of single layers (i.e. layers spaced by more than 7 Å) and a larger interlayer spacing. This suggests a strong development of slit-shaped pores.

Theoretical studies were performed by Duber *et al* [5] to specify the role of the porosity and of the pore morphology of carbon materials, on their bireflectance. According to the pore morphology, different types of anisotropy can be obtained from a pure negative uniaxial graphite crystal to biaxial carbon materials. These models show that the

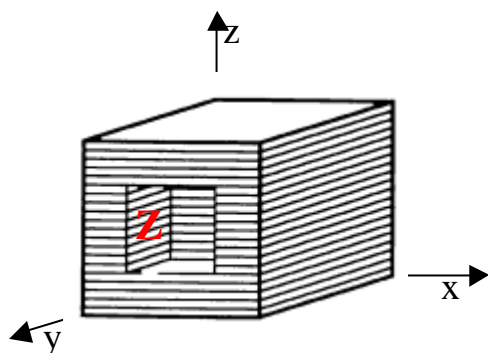


Figure 8. Model of slit-shaped porous carbon (from [6]).  
Z represents the pore height

maximum reflectance decrease as the porosity increase. A microtextural model of slit-shaped pore is shown in the figure 8 (the lines correspond to the profile of the aromatic layers) and different pore size dimensions (x,y,z) varying between 0 and 1 can be obtained from a elementary cubic unit. This model is, up to now, the more appropriated to reproduce the evolution of the optical data versus the porosity increase. This is demonstrated by the figure 9 where  $x=y=0.5$ . The decrease of  $R_{ev}$  according to z, the pore height, is quite similar to the one found for our true carbon materials (see Figure 7). This suggests that information on porosity of carbon materials could be relatively easily obtained from such optical data.

Pertinent quantitative structural and microtextural data are still required to a better understanding of the adsorption properties of such porous carbons and, consequently to fit their application in the environment or in the energy fields (storage capacities).

## References

1. Rouzaud JN, Galvez A, Beyssac O, Fontugne, C, Clinard, C and Goffé B, in : Prospect for Coal Science in the 21<sup>st</sup> Century , B.Q. Li & Z.Y. Liu Eds, Shanxi Sci. & Techn Press, 1999, Vol. 1, p. 25-28.
2. Clinard C, Rouzaud JN and Pellenq JM. Extended Abstracts VIM 2001 (Visualisation Image Modelisation), Nancy, (France): 2001, in press.
3. Kilby WE. Int. J. Coal Geology, 1988;9:267-285
4. Duber S, Pusz S, Kwiecińska BK, Rouzaud, J.N., Intern. J. Coal Geol., 2000;44:227-250.
5. Duber S and Rouzaud JN.. Int. J. Coal Geology, 1999;38:333-348.
6. Jagtoyen M, Derbyshire F, Rimmer S and Rathbone R. Fuel 1995;74: 610-614.

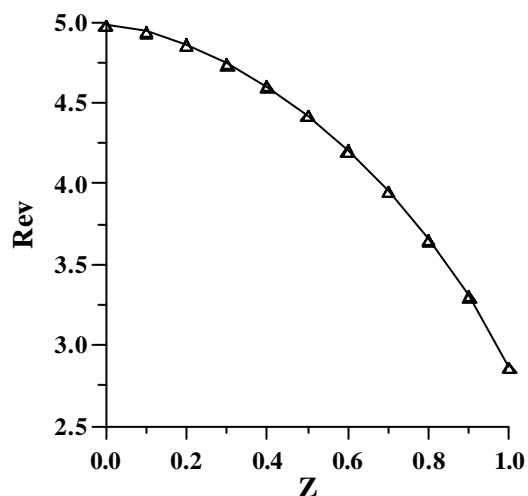


Figure 9. Evolution of  $R_{ev}$  calculated for the Figure 8 model (with  $x=y=0.5$ ) versus Z, the pore height (from [6]).